A model for the global variation in oceanic depth and heat flow with lithospheric age

Carol A. Stein* & Seth Stein†

* Department of Geological Sciences, University of Illinois at Chicago, Chicago, Illinois 60680, USA
† Department of Geological Sciences, Northwestern University, Evanston, Illinois 60208, USA

Variations in sea-floor depth and heat flow with age provide the main constraints on the thermal structure and evolution of the oceanic lithosphere. Joint fitting of heat flow and bathymetry yields a model with a hotter, thinner lithosphere than in previous models. The new model provides a significantly better fit to the data, including those from older lithosphere previously treated as anomalous. This will facilitate the analysis of lithospheric processes, including the effects of mid-plate volcanism and swells, regional subsidence, and hydrothermal circulation near spreading centres.

THE plate tectonic cycle, in which oceanic lithosphere cools as it spreads away from mid-ocean ridges and is reheated on returning to the mantle at subduction zones, is a surface manifestation of terrestrial convection[1-3] and the primary mode of heat transfer from the Earth's interior[4-6]. The resulting thermal evolution of the oceanic lithosphere governs its properties as a function of age and hence the style of plate tectonics.

Following the realization that sea-floor heat flow is highest at mid-ocean ridges and decreases with distance[7-9], the systematic variation of ocean depth and heat flow with age (Fig. 1) became the primary constraint on models of the thermal evolution of the lithosphere. The two sets of data jointly reflect the evolution with age of the geotherm in the lithosphere, because the bathymetry depends on the temperature integrated over depth and the heat flow depends on the temperature gradient at the sea floor[10,11]. The key features of the data, the decrease in heat flow and increase in sea-floor depth with age, prompted two classes of models describing how lithosphere cools as it spreads away from ridges. Each model predicts the variation in depth and heat flow with age. In one model[10], the lithosphere behaves as the cold upper boundary layer of a cooling halfspace, such that the depth and heat flow vary as $age^{1/2}$ and $age^{-1/2}$, respectively. In the other model, the lithosphere is treated as a cooling plate with an isothermal lower boundary[8,11], and so behaves as a cooling boundary layer until it reaches ages at which the effects of the lower boundary cause the depth and heat flow curves to flatten and vary more slowly with age. The plate thickness in the model is the asymptotic thermal thickness approached by old lithosphere, which presumably reflects the combined effects of temperature and rheology[1]. Parsons and Sclater[12] found that such a model, for a 125-km-thick plate with a basal temperature of 1,350 °C, provided good fits to the data then available. It describes the general shape of the depth curve, including the flattening for ages >70 Myr and the heat flow for ages >50 Myr. Its main limitation, the overprediction of heat flow for ages <50 Myr, is thought to result from the transport of significant amounts of heat by water circulation[13], rather than by the conductive cooling assumed in such models.

The simplicity and ease of computation of the plate model makes it a useful representation for the global average of depth and heat flow with age, and for the thermal evolution of the lithosphere. The model's key feature, the isothermal base of the lithosphere, is a simple way of describing the additional heat assumed to prevent the halfspace cooling from continuing for older ages. Various mechanisms including radiogenic heat[14], shear heating[15], small-scale convection[1,16] and mantle plumes[17-19] have been proposed as sources of the additional heat. In most of these formulations, the asymptotic thickness to which the lithosphere evolves corresponds to the depth at which

the additional heat is supplied, and above which the temperature changes cause bathymetric variations. Because the thermal structure within the lithosphere does not depend critically on how this heat is supplied[16], the plate model is a standard for comparing the predicted temperatures within the lithosphere to data including seismic wave velocities[20], flexure due to applied loads[21,22] and the depths of intraplate earthquakes[23].
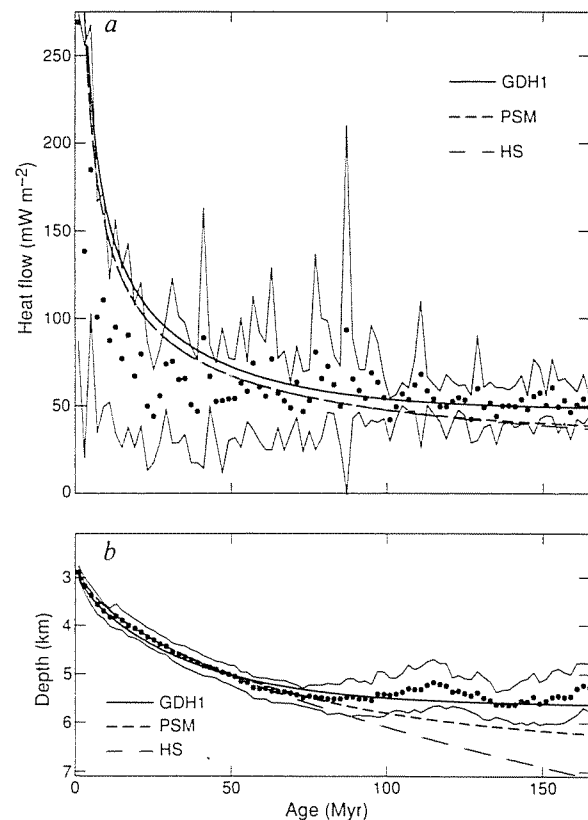

FIG. 1 Data and models for (a) heat flow and (b) ocean depth as a function of age. Depths are an average of North Pacific[24] (north of the Equator) and Northwest Atlantic[25] (15° N–45° N, 40° W–80° W) values; heat flow are from sites (Fig. 2) in these regions. The data are averaged in 2-Myr bins, and one standard deviation about the mean value for each is shown by the envelope. Shown are the plate model of Parsons and Sclater[12] (PSM), a cooling halfspace model with the same thermal parameters (HS) and the GDH1 plate model derived here. In a, the HS and PSM curves overlap for ages younger than ~120 Myr.

Much attention has been directed to depth[24,25] and heat flow[26,27] anomalies relative to the Parsons and Sclater model (a term used for a plate model with the parameters they estimated from the data), to identify processes not adequately described by the model. These studies have been impeded because this model, which we refer to as PSM, predicts deeper depths and lower heat flow than generally observed for lithosphere older than 70–100 Myr (Fig. 1). In particular, these biases pose difficulties for identifying possible mid-plate thermal perturbations due to mantle plumes[28,29].

To address these difficulties, we combine the depth and heat flow data to estimate suitable parameters for plate models. Largely by using improved heat-flow data, we find that a plate model with a hotter and thinner lithosphere (1,450 °C at the base of a 95-km-thick plate) satisfies many of the data that are anomalous with respect to PSM.

Data analysis

We used a heat-flow data set considerably larger than that available to Parsons and Sclater. Of the 5,539 data, 4,217 are from a published compilation[30], and the remainder, some of which have been reported elsewhere[29], are from one in preparation by D. Abbott and C.A.S. The data provide good coverage of the main ocean plates (Fig. 2). We used only good-quality experimental data, as defined in ref. 29, and excluded data from marginal basins, whose thermal evolution may differ from that of larger oceanic plates[31]. The data are at sites younger than 166 Myr, the oldest at which magnetic anomalies provide ages. Because the heat flow and depth for old lithosphere provide joint constraints, we derived the model using only data (Fig. 1) from the North Pacific and Northwest Atlantic, where the published depth data extend to at least 166 Myr and have been corrected for sediment thicknesses.

We initially compared the data to the heat flow and depth predicted by PSM and a halfspace model. In plate models[11,12], the temperature as a function of distance x from the ridge and depth z below the sea floor is given by

$$T(x, z) = T_m \left[z/a + \sum_{n=1}^{\infty} c_n \exp(-\beta_n x/a) \sin(n\pi z/a) \right]$$

where the asymptotic thermal plate thickness is a, its basal temperature is T_m and

$$c_n = 2/(n\pi), \qquad \beta_n = (R^2 + n^2\pi^2)^{1/2} - R, \qquad R = va/(2\kappa)$$

As this expression is in terms of depth rather than height above the plate base, it differs slightly from that in ref. 12. The Peclet number R, relating the advective and conductive heat transfer, incorporates the half spreading rate v and the thermal diffusivity $\kappa = k/(\rho_m C_p)$, where k is thermal conductivity, ρ_m is mantle density and C_p is specific heat. The corresponding heat flow is

$$q(x) = k \left(\frac{\partial T}{\partial z}\right)_{z=0} = q_s \left[1 + 2 \sum_{n=1}^{\infty} \exp(-\beta_n x/a) \right]$$

where $q_s = kT_m/a$ is the asymptotic heat flow for old lithosphere, in which the thermal gradient is linear. The ocean depth varies with distance as

$$d(x) = d_r + d_s \left[1 - \frac{8}{\pi^2} \sum_{j=1}^{\infty} j^{-2} \exp(-\beta_j x/a) \right]$$

$$d_s = \frac{\alpha \rho_m T_m a}{2(\rho_m - \rho_w)}$$

where j takes only odd values, d_r is the depth of the ridge axis, d_s is the asymptotic subsidence for old lithosphere, α is the volume coefficient of thermal expansion and ρ_w is the water density. We refer ocean depths to the ridge axis, rather than to the less easily identified asymptotic depth for old lithosphere. For sufficiently young ages, a plate model is indistinguishable from a cooling halfspace model[10], in which for age t the temperature is

$$T(t, z) = T_m \, \mathrm{erf}\,(z(4\kappa t)^{-1/2})$$

the heat flow is

$$q(t) = kT_m(\pi\kappa t)^{-1/2}$$

and the depth is given by

$$d(t) = d_r + 2(\kappa t/\pi)^{1/2} \alpha \rho_m T_m/(\rho_m - \rho_w)$$

The predictions shown (Fig. 1) are for the parameters used in PSM, a 125-km-thick plate with a basal temperature of 1,350 °C, coefficient of thermal expansion 3.28×10^{-5} K^{-1}, specific heat 1.171 kJ kg^{-1} K^{-1} (0.28 cal g^{-1} K^{-1}), conductivity

a Global heat-flow data

FIG. 2 Locations and lithospheric ages of the heat-flow data. North Pacific and Northwest Atlantic data (Fig. 1) were used to derive the GDH1 model; all the data are used in Fig. 4a and b.
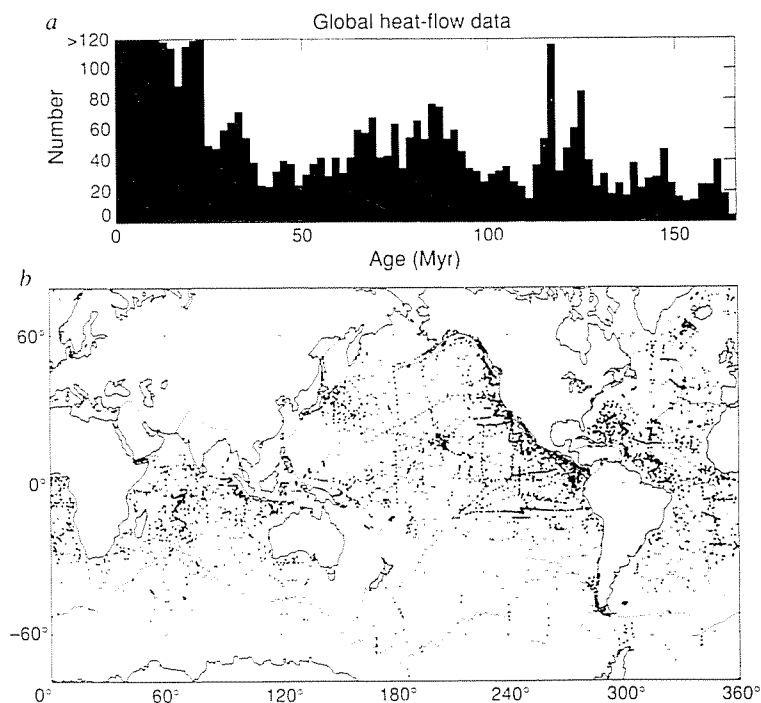
FIG. 3 *a–e*, Contour plots of the misfit to subsets of the data as a function of combinations of the three parameters. In each panel, the best fit is denoted by a cross, and the contours show values 1.25 and 2.5 times the minimum misfit. Parsons and Sclater's values (PSM) and their estimated uncertainties are also indicated. The best-fitting solution for the combined depth and heat flow (*c–e*), a 95-km-thick plate with a basal temperature of 1,450 °C and coefficient of thermal expansion 3.1×10^{-5} K^{-1}, is model GDH1. *f*, Misfit to the data for GDH1, PSM, the halfspace model and a version of the PSM model including radioactivity (arrow), which predicts the same depths but higher heat flow than PSM.
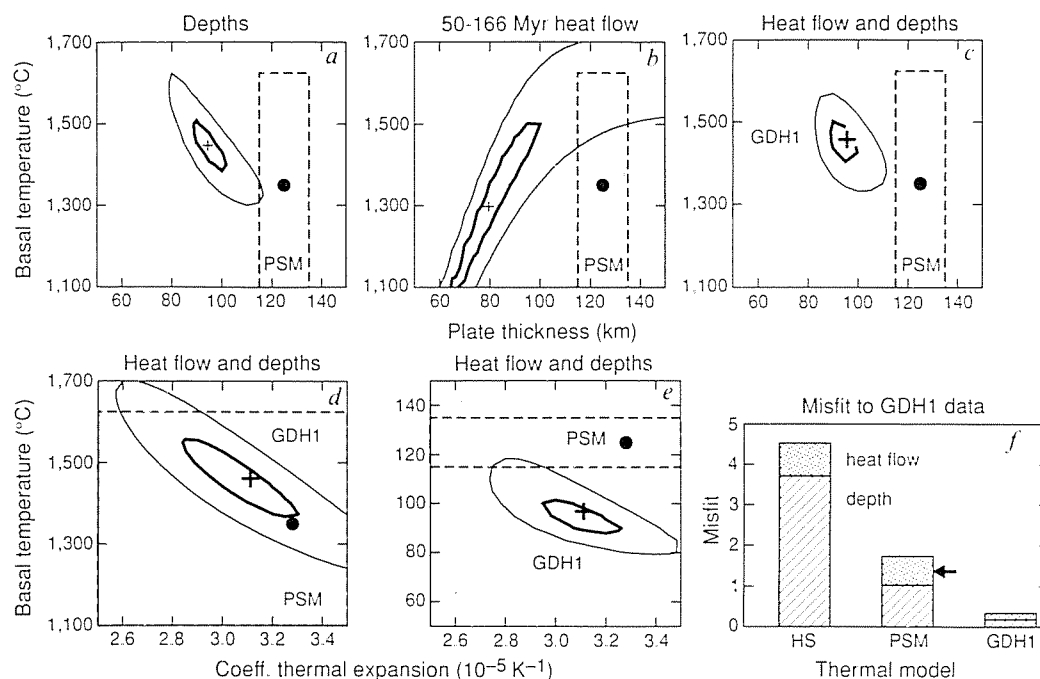
3.138 W m^{-1} K^{-1} (7.5×10^{-3} cal K^{-1} cm^{-1} s^{-1}), mantle density $3,330$ kg m^{-3}, water density $1,000$ kg m^{-3} and ridge depth $2,500$ m, and for a halfspace model with the same thermal parameters and ridge depth. The predicted depths for PSM flatten with respect to the halfspace model for ages >70 Myr, whereas the predicted heat flow differs from that for the halfspace only slightly for large (>140 Myr) ages, because the bottom boundary condition influences the integrated temperature at an age younger than that at which its effect reaches the surface.

It is useful to separate the data into four categories. The heat flow data can be divided into ages younger or older than ~ 50–75 Myr. The data for younger ages are not fitted by the conductive models, presumably because of hydrothermal circulation[13]. The heat flow for older ages changes slowly with age, such that with our data the slope is not resolvably different from zero for ages greater than 80–90 Myr, and the average values systematically exceed those predicted by PSM[26–29,32]. Similarly, the depth data behave differently for ages younger or older than 40–70 Myr. Younger values are reasonably well fitted by either PSM, other plate models, or halfspace models, whereas the older depths are generally overpredicted by PSM, as previously noted[24,25,29,33–36].

We investigated how well the data were fitted by plate models with different lithospheric thicknesses, basal temperatures and coefficients of thermal expansion. We considered the combined misfit to the depth and heat-flow data

$$s^2(a, T_m, \alpha) = s_d^2 + s_q^2 = \frac{1}{N} \sum_{i=1}^{N} (d_i - \hat{d}_i)^2 / \sigma_{d_i}^2$$

$$+ \frac{1}{M} \sum_{j=1}^{M} (q_j - \hat{q}_j)^2 / \sigma_{q_j}^2$$

where d_i and $\hat{d}_i$ are the observed and predicted depths in the ith age interval, σ_{d_i} is the standard deviation of the depth for this interval, and q_j, $\hat{q}_j$ and σ_{q_j} are the corresponding heat flow quantities. We used the PSM values for the other parameters, except for a slightly deeper ridge depth of 2,600 m, in keeping with recent data[34,36]. Our approach of treating the depth and heat flow as joint constraints is conceptually similar to Parsons and Sclater's, differing primarily in that the data are sufficiently densely sampled to permit numerical fitting.

We calculated the misfit at increments of 5 km in plate thickness, 25 K in basal temperature and 5×10^{-7} K^{-1} in coefficient of thermal expansion. Figure 3*a–c* shows contours of the misfit as a function of basal temperature and thickness, for the best-fitting coefficient of thermal expansion, 3.1×10^{-5} K^{-1}. These plots show a slice of the three-dimensional model space with α fixed. Figure 3*d* shows the misfit as a function of the coefficient of thermal expansion and basal temperature, for the best-fitting thickness of 95 km, and Fig. 3*e* shows the misfit as a function of the coefficient of thermal expansion and thickness, for the best-fitting basal temperature, 1,450 °C.

The misfit contours for the depths show a diagonal pattern because the asymptotic depth is proportional to the product of plate thickness and basal temperature. The best fit is for a thinner plate and higher temperature than in PSM, consistent with the observed depths (Fig. 1) being shallower than predicted by PSM. The heat-flow data for lithosphere older than 50 Myr provide a separate constraint. The misfit contours are elongated diagonally in the opposite sense as for the depths, because the asymptotic heat flow depends on the ratio of basal temperature to thickness. As for the depths, the best fit occurs for a thinner plate and higher T_m/a than for PSM, because the observed heat flow exceeds that predicted by PSM. The coefficient of thermal expansion plots show the best fitting value, and the partial tradeoffs because the depths for young and old ages depend on the products αT_m and $\alpha T_m a$, respectively. Joint fitting of the combined depth and heat flow data gives a best fit for a 95-km-thick plate, with a basal temperature of 1,450 °C, coefficient of thermal expansion, 3.1×10^{-5} K^{-1}, and all other parameters except the ridge depth the same as for PSM.

This model, which we call GDH1 (for global depth and heat flow), fits the data considerably better than PSM, especially for old lithosphere (Fig. 1). GDH1 predicts an asymptotic depth for old lithosphere of 5,651 m, considerably shallower than the 6,400 m for PSM. The asymptotic heat flow for GDH1 is 48 mW m^{-2}, roughly 40% higher than the value of 34 mW m^{-2} for PSM. As a result, the depth and heat flow misfits for GDH1 are $s_d^2 = 0.18$ and $s_q^2 = 0.16$, whereas the corresponding misfits for PSM are substantially higher, 1.01 and 0.70. An F-ratio test indicates that the improved fit is significant above the 99.9% level. Figure 3*f* shows that the improved fit of GDH1 relative to PSM is comparable to that for PSM relative to the halfspace model. An F-ratio test shows that GDH1 also provides an

improved fit above the 99.9% level relative to a version of the PSM model in which, in addition to the heat flow due to plate cooling, 4 mW m^{-2} is assumed to be generated by radioactivity[12], giving the same depths as PSM but a better fit to the heat flow ($s_q^2 = 0.34$).

A range of models gives fairly similar curves of depth and heat flow against age. For example, if we assume the PSM value for the coefficient of thermal expansion, we obtain a best-fitting thickness of 95 km and a basal temperature of 1400 °C. Alternatively, varying both thermal conductivity and α yields a best fit for k of 3.25 W m^{-1} K^{-1}, α of 3.1×10^{-5} K^{-1}, a thickness of 95 km and T_m of 1,425 °C. An F-ratio test shows that the improved fit from estimating the conductivity from the data is not significant even at the 90% level, because the resulting value is similar to that previously assumed. It is, however, gratifying that solving for the conductivity gives a value consistent with that usually assumed. Different choices of data also yield similar best-fitting parameters. For example, use of the heat-flow data for ages older than 75 Myr, rather than 50 Myr, yields a best fit for a thickness of 95 km, T_m of 1,475 °C and α of 3.05×10^{-5} K^{-1}. This model is so similar to GDH1 that it predicts an asymptotic heat flow within 1 mW m^{-2} and an asymptotic subsidence within 3 m of those for GDH1.

GDH1 is thus representative of the plate models that fit the data well. Quantification of the true uncertainties in model
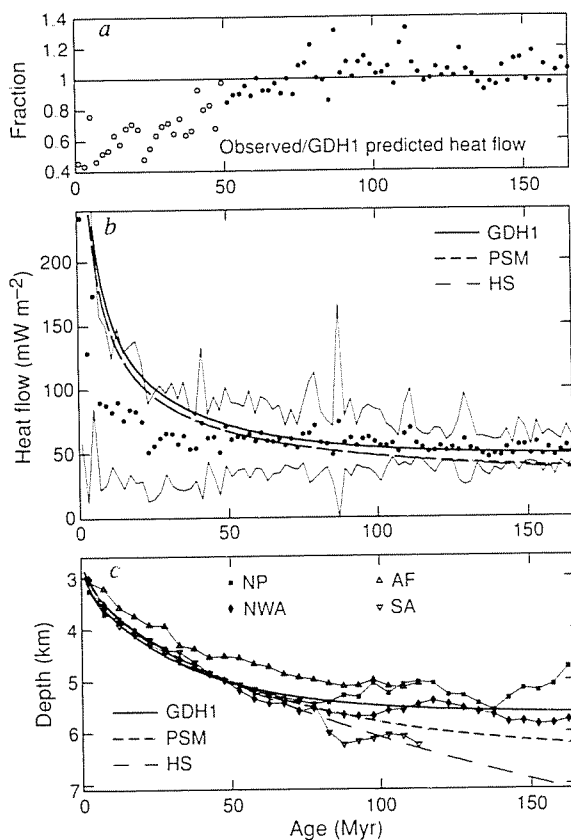

FIG. 4. Use of GDH1 as a reference model for depth and heat-flow analyses. a, Observed heat flow against age for the entire global dataset as a fraction of that predicted by GDH1. The discrepancy for ages younger than 50–75 Myr presumably indicates the fraction of the heat transported by hydrothermal flow. The data for ages <50 Myr (open circles) were not used in deriving GDH1. b, Observed heat against age for the entire global dataset, and predictions of PSM, a halfspace model with the same thermal parameters (HS) and GDH1. The HS and PSM curves overlap for ages younger than ~120 Myr. Symbols are the same as in Fig. 1. c, Depth data (averaged in 5-Myr bins) for the South American (SA)[46] and African (AF)[46] plates, and the North Pacific (NP)[24] and Northwest Atlantic (NWA)[25] compared to the predictions of the three models. The differences between plates make any global reference model only an approximation.

parameters is difficult, given the limitations of the data and model (discussed later). From examination of fits to the data, we estimate the plate thickness as 95 ± 15 km, basal temperature as $1,450 \pm 250$ °C and α as $3.1 \pm 0.8 \times 10^{-5}$ K^{-1}, where the uncertainties are one standard deviation, and do not include the uncertainty in the model or other parameters (such as conductivity). Alternatively, if we regard α as known a priori, we estimate the thickness and T_m uncertainties as 10 km and 100 °C, respectively. Thus our solutions have plate thicknesses generally less than Parsons and Sclater's estimate (125 ± 10 km), basal temperatures comparable to their estimate ($1,350 \pm 275$ °C) and α comparable to their estimate ($3.2 \pm 1.1 \times 10^{-5}$ K^{-1}).

Applications of the model

Thermal models of the lithosphere are used in several ways for tectonic studies. First, they provide reference models to characterize the average variation in depth and heat flow with age for assumed 'normal' lithosphere. It is thus possible to identify regions that are anomalous with respect to a reference model, and to estimate how anomalous the depth and heat flow are. Second, a model predicts a geotherm for 'normal' lithosphere, and hence can be used to draw inferences about the processes giving rise to the temperature structure of both 'normal' and 'anomalous' lithosphere. These two applications are decoupled, in that it is useful to characterize 'normal' lithosphere and identify anomalies, although the assumed thermal structure presumably approximates a more complex situation.

GDH1 is a more useful global reference model than PSM, as it fits many of the data better for old lithosphere. It avoids the difficulty that most old lithosphere seems anomalous relative to PSM. The fact that many previously inferred heat flow and depth anomalies are successfully described by a single model bears out the importance of using both data types to constrain models.

The depth and heat-flow predictions for GDH1 are conveniently and accurately approximated using a halfspace model with the same parameters for young lithosphere, and the first term of the series solution with $R \gg \pi$ for older lithosphere[12]. The depth (m) is related to the age (Myr) by

$$d(t) = 2,600 + 365\, t^{1/2} \qquad t < 20 \text{ Myr}$$

$$\left.\begin{array}{l} = d_r + d_s[1 - (8/\pi^2)\exp(-\kappa\pi^2 t/a^2)] \\ = 5,651 - 2,473\exp(-0.0278t) \end{array}\right\} \quad t \geqslant 20 \text{ Myr}$$

and the heat flow (mW m^{-2}) is

$$q(t) = 510 t^{-1/2} \qquad t \leqslant 55 \text{ Myr}$$

$$\left.\begin{array}{l} = q_s[1 + 2\exp(-\kappa\pi^2 t/a^2)] \\ = 48 + 96\exp(-0.0278t) \end{array}\right\} \quad t > 55 \text{ Myr}$$

Hotspot swells. The GDH1 predictions are useful for investigation of the depth and heat-flow anomalies at swells associated with presumed hotspots. Two common end-member models for the swells are a thermal origin, in which the lithosphere is reheated at depth[37,38], or a dynamic origin, in which upwelling mantle causes uplift[39–41]. The observation of heat flow along the Hawaiian swell higher than predicted for PSM was initially treated as consistent with reheating[38], because this model predicts large heat-flow anomalies. Subsequent studies showed that swell heat flow differs at most slightly from that for lithosphere of comparable ages[28], so that referring the data to PSM overestimated the anomalies. GDH1 fits the global heat-flow data (only part of which was used in deriving the model) significantly better than PSM (Fig. 4b) and is therefore a more appropriate reference. Thus although relative to PSM the anomaly is ~6–10 mW m^{-2} (depending on whether radioactivity is assumed), the anomaly relative to GDH1 is ~4 mW m^{-2}. The heat-flow anomalies over the other swells are similarly reduced, thus favouring dynamic rather than reheating models, in accord with recent seismological results[42].
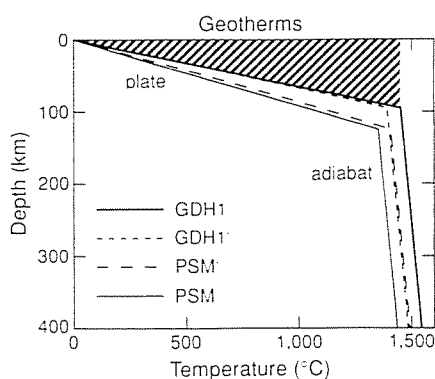
FIG. 5 Comparison of the asymptotic thermal structure for old lithosphere in models PSM and GDH1. GDH1, developed to fit higher heat flow, has a steeper geotherm and thus higher temperatures at depth. The sea-floor subsidence is proportional to the area (shaded) between the geotherm and $T = T_m$, so GDH1 predicts less subsidence and hence shallower bathymetry than PSM. Versions of these models incorporating the effect of radioactivity are labelled GDH1′ and PSM′. Schematic adiabats are shown beneath the plate.

Hydrothermal circulation. A reference model like GDH1 can be used to study hydrothermal circulation in young lithosphere[13,43,44]. Comparison of the observed conductive flux to that predicted (Fig. 4a) suggests that the fraction of heat transferred by fluid flow decreases steadily from less than ~50% in very young lithosphere. GDH1 slightly underpredicts the heat flow for old lithosphere, perhaps in part because it is also constrained by the depths (Fig. 3).

Depth anomalies. Although a reference model is needed to identify and characterize depth anomalies, the differences in subsidence rates between plates (Fig. 4c) and within plates are substantial enough[10,34,45,46] that no model can fit all the data. Similarly, our fitting of mean depths, which are convenient for statistical analysis, or the alternative of fitting modal depths, which are less affected by processes that produce shallow depths[24], affects the result. Any global reference model is therefore an approximation to an ideal. Nonetheless, comparison with either mean or modal depths shows that GDH1 is a more useful reference than PSM, which has the unsatisfying implication that most older lithosphere is anomalously shallow. Moreover, the approach used to derive GDH1 may be applied to differences between and within plates. Although such analyses have often considered only depths and interpreted the differences in terms of temperature variations[46], it may sometimes be practical to use both data types and also test different plate thicknesses. Although the data for young lithosphere are insensitive to plate thickness and hence describable by halfspace cooling, the data for older lithosphere are sensitive to plate thickness. It would also be desirable to derive a revised global model, using sediment-corrected depth data for old lithosphere from other areas (such as the Indian Ocean and Northeast Atlantic).

Because GDH1 is derived by joint fitting of bathymetry and heat-flow data, both the depths and heat flow are assumed to reflect thermal structure. Regions anomalous with respect to the model can thus be characterized in terms of two end-member cases, thermally or topographically anomalous. The former situation (anomalously shallow bathymetry and high heat flow) presumably reflects temperatures in the lithosphere higher than in GDH1. In contrast, the latter situation (regions shallow with respect to GDH1, but with consistent heat flow) may reflect dynamic uplift, excess volcanism or thick crust. The small heat-flow anomaly associated with Hawaii and the other hotspot swells indicates that they are closer to this second case.

An important use of depth data is for analysis of the history of old lithosphere[47]. The observation that old lithosphere is shallow with respect to a halfspace model gave rise to the plate model, which fits most of the data reasonably well and is thus the standard reference. The issue is generally not whether a given region of old lithosphere is anomalous relative to a cooling halfspace, because this is almost always the case, but whether it is shallow relative to old lithosphere of comparable age elsewhere[29]. Despite the variations in the depth for a given age, such that 'flattening' is only an approximation, GDH1 describes most old lithosphere better than PSM. Thus the regions for ages

>100 Myr (primarily in the Pacific) which are anomalously shallow with respect to PSM (Figs 1, 4c) are either consistent with or considerably less shallow with respect to GDH1.

GDH1 or any reference model is thus helpful in investigating the physical process causing the flattening with respect to the square root of age curve. A reference model characterizes the average heat flow and depth values as a function of age, which models of the physical process must satisfy. Many recent studies favour hotspot reheating, in part because of questions about whether small-scale convection would cause flattening[3,19]. If the flattening is caused by hotspots, therefore, a plate model like GDH1 describes their average effect, and regions shallow with respect to GDH1 (such as Hawaii) have been affected more than 'normal' old lithosphere.

Thermal structure of the lithosphere

The difference between the predicted temperature structure of the lithosphere for GDH1 and PSM can be visualized using the asymptotic thermal structure for old lithosphere (Fig. 5), a linear geotherm, $T_m z/a = q_s z/k$. The age at which the geotherm becomes roughly linear corresponds to that at which the predicted heat flow becomes roughly uniform with age: ~100 Myr for GDH1 and ~150 Myr for PSM. The geotherm is easily interpreted graphically, because the physical properties are assumed to be uniform with depth. The surface heat flow constrains the slope of the geotherm. The geotherms for PSM and GDH1 can be compared directly because the models have the same conductivity. GDH1, with higher heat flow than PSM, has a steeper gradient and higher temperature at any depth. The observed subsidence constrains the area between the geotherm and $T = T_m$, which is proportional to $T_m a$ and thus to the heat lost as the plate cools from its initial temperature. The area between the geotherm and the depth axis is proportional to the heat remaining in the lithosphere, the vertical integral of temperature. For the linear gradient, the two areas are equal, so half of the initial heat has been lost. GDH1, derived for shallower bathymetry and hence less subsidence than PSM, has a smaller area between the geotherm and $T = T_m$. The model makes no predictions about the temperatures below the plate, often assumed to be a shallow adiabatic gradient, ~0.3 °C km^{-1} (ref. 48). Given the simplifying assumptions and uncertainties, the temperatures at depth are in reasonable accord (±100 K) with those inferred from mineral physics[49].

Beyond the general properties that GDH1 is hotter at depth and has a thinner asymptotic thermal plate than PSM, we do not ascribe great significance to the details of the temperature structure, especially the basal temperature and the thermal structure in the lower portions of the plate. Plate models are phenomenological in that they are the simplest models (specified by the minimum number of parameters) that describe the general variation in depth and heat flow. These variations may reflect potentially significant effects not included in the model. For example, the basal temperature depends on whether the model incorporates radiogenic heat production, as illustrated by the

asymptotic geotherm $T(z) = q_s z/k - Hz^2/(2k)$, where H is the heat production per unit volume[48]. Geotherm GDH1' (Fig. 5) shows that for a typically assumed heat production of 10^{-14} cal s cm^{-3} (4.184×10^{-8} W m^{-3})[9,20], the basal temperature would be reduced to 1,393 °C. Conversely, because in deriving PSM[12] it was assumed that an additional ~4 mW m^{-2} of asymptotic heat flow was due to radioactivity, addition of this effect would give geotherm PSM', with a basal temperature of 1,409 °C. Because the basal temperature depends on the poorly known heat production, we have not complicated the GDH1 model by including this effect.

Other factors contribute to the uncertainty in the basal temperature. A depth dependent coefficient of thermal expansion[20] or conductivity[50] could have considerable effects. Because we use no heat-flow data in lithosphere younger than 50 Myr, we accept a boundary condition at the ridge which gives a heat-flow singularity that a more physical boundary condition can alleviate[5,10,51]. Moreover, the temperatures at shallow depths in very young lithosphere are presumably lowered by hydrothermal circulation[44]. The model includes only the variation in the depth due to the cooling lithosphere[16], whereas large- and small-scale convection[2,3,52], temperature variations within the mantle, and phase changes[53] may also yield depth effects. The model does not incorporate time-dependent effects apart from cooling, as might be associated with processes like the proposed Cretaceous superplume[54].

Determination of the magnitude of effects not included in the plate model is challenging because the model fits the primary surface observables, depth and heat flow, reasonably well. A final point worth noting is that in the plate model, the ridge and basal temperatures are treated as the same for simplicity. These temperatures are presumably different, in that the basal temperature represents the heat addition to old lithosphere. If this addition occurs through mantle plumes, the basal temperature would be expected to be several hundred degrees higher than the ridge temperature[55]. This may be the reason why the basal temperature exceeds that (~1,300 °C) inferred for the ridge temperature from the thickness of oceanic crust[61,62].

In addition to the surface observables, the thermal evolution of the lithosphere seems to give rise to variations with age of properties at depth, as inferred from surface-wave velocities[20,56,57], effective elastic thicknesses[21,22] and the maximum depth of seismicity[23,58]. It is hard to use these variations to discriminate between grossly similar thermal models like PSM and GDH1 (Fig. 6) because the predicted temperatures are similar at shallow depths, especially for young lithosphere. The inferred temperatures of ~400 °C associated with the effective elastic thickness[21] (except for the South Pacific superswell[59]) and of ~750 °C corresponding to the deepest intraplate seismicity[23] occur at similar depths for PSM and GDH1, except for old lithosphere. More detailed comparison of these data with predicted temperature structures requires rheological models and assumptions about the relevant strengths. The velocity structure inferred from surface-wave dispersion might be more diagnostic because the low-velocity zone occurs at greater depth, where predicted temperature differ more. Laboratory experiments[60] indicate that the velocity should begin to decrease at a depth where the temperature is ~95% of the solidus temperature. Unfortunately, even with this assumption the velocity structure is difficult to relate in detail to thermal models because of the limited vertical and age resolution of the dispersion data[20,56,57]. For the velocity structure shown, however, the inception of the low-velocity zone occurs at shallower depths in older lithosphere than would be expected for the present solidus data[60], either for PSM or the hotter GDH1.

The GDH1 model provides a convenient reference for the average variation in depth and heat flow with lithospheric age. It can be used in studying these surface observables, regardless of how well the plate model actually represents the thermal structure of the lithosphere. If a plate model adequately represents the geotherm, GDH1 implies that the lithosphere is hotter at depth and thinner than previously assumed. ☐
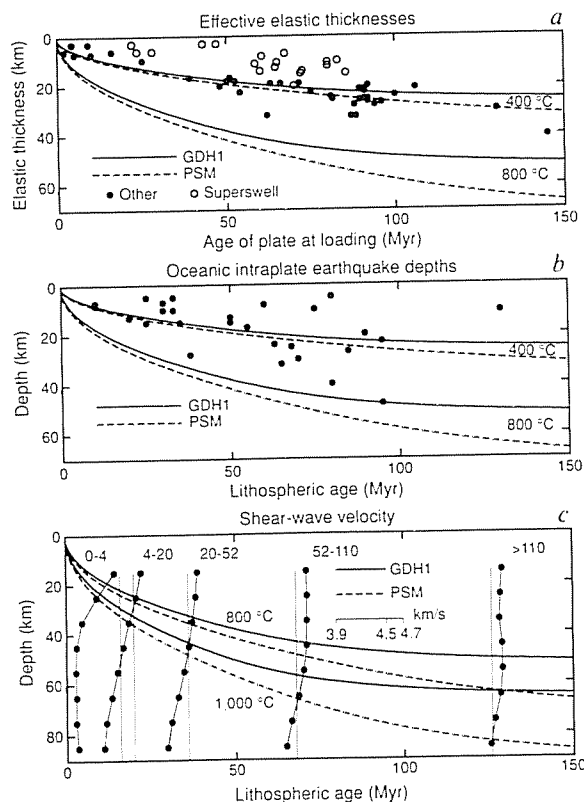

FIG. 6 Comparison of the isotherms as a function of age for the PSM and GDH1 models to three data sets[22,23,56] whose variation with age is consistent with cooling of the lithosphere. Except for the oldest lithosphere, the isotherms corresponding to the effective elastic thickness (a) and deepest intraplate seismicity (b) are similar for the two models. The difference between the temperatures for the low-velocity zone (c) is greater. The vertical line for the velocity structure in each age range (for example 0–4 Myr) corresponds to 4.5 km s^{-1}.

1. Parsons, B. & Richter, F. M. in *The Sea 7* (ed. Emiliani, C.) 73–117 (Wiley, New York, 1981).
2. Jarvis, G. T. & Peltier, W. R. in *Mantle Convection* (ed. Peltier, W. R.) 479–594 (Gordon and Breach, New York, 1989).
3. O'Connell, R. J. & Hager, B. H. in *Physics of the Earth's Interior. Proc. int. Sch. Phys. "Enrico Fermi"* (eds Dziewonski, A. M. & Boschi, E.) 270–317 (North-Holland, Amsterdam, 1980).
4. Chapman, D. S. & Pollack, H. N. *Earth planet. Sci. Lett.* **28**, 23–32 (1975).
5. Sclater, J. G., Jaupart, C. & Galson, D. *Rev. Geophys. Space Phys.* **18**, 269–311 (1980).
6. Davies, G. F. *Rev. Geophys. Space Phys.* **18**, 718–722 (1980).
7. Von Herzen, R. P. & Uyeda, S. *J. geophys. Res.* **68**, 4219–4250 (1963).
8. Langseth, M. G., Le Pichon, X. & Ewing, M. *J. geophys. Res.* **71**, 5321–5355 (1966).
9. Sclater, J. G. & Francheteau, J. *Geophys. J. R. astr. Soc.* **20**, 509–542 (1970).
10. Davis, E. E. & Lister, C. R. B. *Earth planet. Sci. Lett.* **21**, 405–413 (1974).
11. McKenzie, D. P. *J. geophys. Res.* **72**, 6261–6273 (1967).
12. Parsons, B. & Sclater, J. G. *J. geophys. Res.* **82**, 803–827 (1977).
13. Anderson, R. N. & Hobart, M. A. *J. geophys. Res.* **81**, 2968–2989 (1976).
14. Crough, S. T. *Phys. Earth planet. Inter.* **14**, 365–377 (1977).
15. Schubert, G., Froidevaux, C. & Yuen, D. A. *J. geophys. Res.* **81**, 3525–3540 (1976).
16. Parsons, B. & McKenzie, D. P. *J. geophys. Res.* **83**, 4485–4496 (1978).
17. Heestand, R. L. & Crough, S. T. *J. geophys. Res.* **86**, 6107–6114 (1981).
18. Schroeder, W. *J. geophys. Res.* **89**, 9873–9883 (1984).
19. Davies, G. F. *J. geophys. Res.* **93**, 10481–10488 (1988).
20. Forsyth, D. W. *Tectonophysics* **38**, 89–118 (1977).
21. Bodine, J. H., Steckler, M. S. & Watts, A. B. *J. geophys. Res.* **86**, 3695–3707 (1981).
22. Calmant, S., Francheteau, J. & Cazenave, A. *Geophys. J. int.* **100**, 59–67 (1990).
23. Wiens, D. A. & Stein, S. *J. geophys. Res.* **88**, 6455–6468 (1983).
24. Renkin, M. L. & Sclater, J. G. *J. geophys. Res.* **93**, 2919–2935 (1988).
25. Sclater, J. G. & Wixon, L. in *The Geology of North America: The Western North Atlantic Region* (eds Vogt, P. R. & Tucholke, B. E.) 257–270 (Geol. Soc. Am. Boulder, 1986).
26. Louden, K. E., Wallace, D. O. & Courtney, R. C. *Earth planet. Sci. Lett.* **83**, 109–122 (1987).
27. Lister, C. R. B., Sclater, J. G., Davis, E. E., Villinger, H. & Nagihara, S. *Geophys. J. int.* **102**, 603–630 (1990).
28. Von Herzen, R. Cordery, P. M. J. Detrick, R. S. & Fang, C. *J. geophys. Res.* **94**, 13783–13799 (1989).
29. Stein, C. & Abbott, D. *J. geophys. Res.* **96**, 16083–16100 (1991).
30. Louden, K. E. in *Handbook of Seafloor Heat Flow* (eds Wright, J. A. & Louden, K. E.) 325–485 (CRC Boca Raton 1989).
31. Uyeda, S. in *Island Arcs Deep-sea Trenches and Back-arc Basins. Maurice Ewing Ser.* 1 (eds Talwani, M. & Pitman, W. C. III) 1–14 (Am. Geophys. Un. Washington DC, 1977).

32. Langseth, M. G., Lachenbruch, A. H. & Marshall, B. V. in *The Geology of North America: The Arctic Ocean Region* (eds Grantz, A., Johnson, L. & Sweeney, J. F.) 133–152 (Geol. Soc. Am. Boulder, 1990).
33. Kaula, W. M. & Philips, R. J. *Geophys. Res. Lett.* **8**, 1187–1190 (1981).
34. Marty, J. C. & Cazenave, A. *Earth planet. Sci. Lett.* **94**, 301–315 (1989).
35. Colin, P. & Fleitout, L. *Geophys. Res. Lett.* **17**, 1961–1964 (1990).
36. Smith, W. H. F. thesis, Columbia Univ. (1990).
37. Detrick, R. S. & Crough, S. T. *J. geophys. Res.* **83**, 1236–1244 (1978).
38. Von Herzen, R. P., Detrick, R. S., Crough, S. T., Epp, D. & Fehn, U. *J. geophys. Res.* **87**, 6711–6723 (1982).
39. Courtney, R. C. & White, R. S. *Geophys. J. R. astr. Soc.* **87**, 815–867 (1986).
40. Robinson, E. M. & Parsons, B. *J. geophys. Res.* **93**, 3144–3156 (1988).
41. Liu, M. & Chase, C. G. *J. geophys. Res.* **94**, 5571–5584 (1989).
42. Woods, M. T., Leveque, J.-J. & Okal, E. A. *Geophys. Res. Lett.* **18**, 105–108 (1991).
43. Sleep, N. H. & Wolery, T. J. *J. geophys. Res.* **83**, 5913–5922 (1978).
44. Lin, J. & Parmentier, E. M. *Geophys. J.* **96**, 1–22 (1989).
45. Cochran, J. R. *Geophys. J. R. astr. Soc.* **87**, 421–454 (1986).
46. Hayes, D. E. *J. geophys. Res.* **93**, 2937–2954 (1988).
47. Sleep, N. H. *J. geophys. Res.* **95**, 21983–21990 (1990).
48. Turcotte, D. L. & Schubert, G. *Geodynamics: Applications of Continuum Physics to Geological Problems* (Wiley New York, 1982).
49. Akaogi, M., Ito, E. & Navrotsky, A. *J. geophys. Res.* **94**, 15671–15685 (1989).
50. Horai, K. & Susaki, J. *Phys. Earth planet. int.* **55**, 292–305 (1989).
51. Sleep, N. H. *J. geophys. Res.* **80**, 4037–4042 (1975).
52. Buck, W. R. & Parmentier, E. M. *J. geophys. Res.* **91**, 1961–1974 (1986).
53. Wood, B. J. & Yuen, D. A. *Earth planet. Sci. Lett.* **66**, 303–314 (1983).
54. Larson, R. L. & Olson, P. *Earth planet. Sci. Lett.* **107**, 437–447 (1991).
55. Sleep, N. H. A. *Rev. Earth planet. Sci.* **20**, 19–43 (1992).
56. Nishimura, C. & Forsyth, D. *Geophys. J.* **96**, 203–226 (1989).
57. Yu, G.-K. & Mitchell, B. *Geophys. J.* **57**, 311–342 (1979).
58. Chen, W.-P. & Molnar, P. *J. geophys. Res.* **88**, 4183–4214 (1983).
59. McNutt, M. K. & Fisher, K. M. in *Seamounts, Islands & Atolls, Geophysical Monograph #43* (eds Keating, B. H. Fryer, P. Batiza, R. & Boehlert, G. W.) 25–34 (Am. Geophys. Un., Washington DC, 1987).
60. Sato H. Sacks, I. S. & Murase, T. *J. geophys. Res.* **94**, 5689–5704 (1989).
61. Sleep, N. H. & Windsley, D. F. *J. Geol.* **90**, 363–379 (1982).
62. McKenzie D. & Bickle, M. J. *J. Petrol.* **29**, 625–679 (1988).